Spatially resolved measurements of nitrogen dioxide in an urban environment using concurrent multi-axis differential optical absorption spectroscopy

R. J. Leigh, G. K. Corlett, U. Friess, P. S. Monks

▶ **To cite this version:**

R. J. Leigh, G. K. Corlett, U. Friess, P. S. Monks. Spatially resolved measurements of nitrogen dioxide in an urban environment using concurrent multi-axis differential optical absorption spectroscopy. Atmospheric Chemistry and Physics Discussions, 2006, 6 (6), pp.12671-12700. hal-00302340

HAL Id: hal-00302340
https://hal.science/hal-00302340

Submitted on 18 Jun 2008

HAL is a multi-disciplinary open access archive for the deposit and dissemination of scientific research documents, whether they are published or not. The documents may come from teaching and research institutions in France or abroad, or from public or private research centers.

L'archive ouverte pluridisciplinaire **HAL**, est destinée au dépôt et à la diffusion de documents scientifiques de niveau recherche, publiés ou non, émanant des établissements d'enseignement et de recherche français ou étrangers, des laboratoires publics ou privés.

Atmos. Chem. Phys. Discuss., 6, 12671–12700, 2006
www.atmos-chem-phys-discuss.net/6/12671/2006/
© Author(s) 2006. This work is licensed
under a Creative Commons License.

Atmospheric Chemistry and Physics Discussions

Spatially resolved measurements of nitrogen dioxide in an urban environment using concurrent multi-axis differential optical absorption spectroscopy

R. J. Leigh[1], G. K. Corlett[1], U. Frieß[1,*], and P. S. Monks[1]

[1]EOS Group, Departments of Chemistry and Physics, University of Leicester, Leicester, UK
[*]now at: University of Heidelberg, Heidelberg, Germany

Received: 17 November 2006 – Accepted: 28 November 2006 – Published: 5 December 2006

Correspondence to: P. S. Monks (p.s.monks@leicester.ac.uk)

Abstract

A novel system using the technique of concurrent multi-axis differential optical absorption spectroscopy system has been developed and applied to the measurement of nitrogen dioxide in an urban environment. Using five fixed telescopes, slant columns of nitrogen dioxide, ozone, water vapour, and the oxygen dimer, O_4, are simultaneously retrieved in five vertically separated viewing directions. The application of this remote sensing technique in the urban environment is explored. Through, the application of several simplifying assumptions a tropospheric concentration of NO_2 is derived and compared with an urban background in-situ chemiluminescence detector. The remote sensing and in-situ techniques show good agreement. Owing to the high time resolution of the measurements, the ability to image and quantify plumes within the urban environment is demonstrated. The CMAX-DOAS measurements provide a useful measure of overall NO_2 concentrations on a city-wide scale.

1 Introduction

Public exposure to nitrogen dioxide (NO_2) in the urban environment is a health concern, a public policy concern and the subject of several national and international directives on air quality. At present monitoring/measurement uses networks of spatially sparse in-situ monitors coupled to emission inventories and empirical models to estimate NO_2 concentrations and exceedences of air quality standards. Considerable spatial inhomogeneity in the dynamics, meteorology and chemistry of the urban atmosphere leaves such techniques open to significant uncertainties unless datasets are available against which they can be rigorously validated. The urban atmosphere therefore presents a substantial measurement and modeling challenge.

Zenith-viewing UV/Visible scattered light differential optical absorption spectroscopy (DOAS) has been used over a number of decades for the retrieval of atmospheric concentrations of traces species including O_3, NO_2, BrO, OClO, IO, HCHO and O_4.

ACPD

6, 12671–12700, 2006

(e.g. Noxon, 1975; Noxon et al., 1979; Solomon et al., 1987; Johnston and McKenzie, 1989; Van Roozendael et al., 1994; Aliwell et al., 2002; Frieß et al., 2001; Wittrock et al., 2000; Tornkvist et al., 2002). In recent years, systems incorporating off-axis (non-zenith) measurements have been developed (e.g. Sanders, 1996; Miller et al., 1997; Hönninger et al., 2004b,c; Bobrowski et al., 2003; Leser et al., 2003; Wittrock et al., 2004; Heckel et al., 2005; Sinreich et al., 2006). Off-axis techniques exploit the improved sensitivity of non-zenith measurements to tropospheric trace-gas concentrations owing to the enhanced tropospheric path length of collected scattered light. Through the incorporation of multiple off-axis viewing geometries, information on the profile and spatial distribution of trace gases can be retrieved.

The DOAS technique can be used to measure absorption by trace species throughout the path length of scattered solar radiation (Platt, 1994). As a general rule the stratospheric path length is modulated by changing solar zenith angle while the tropospheric path length is dominated by changes in instrument viewing geometry (Hönninger et al., 2004a). Tropospheric sensitivity is minimised in the zenith view, as photons are generally scattered in the lower stratosphere and upper troposphere and therefore take a vertical path straight through the boundary layer. Off-axis viewing angles with elevations less than 20 degrees above the horizon have much greater sensitivity to the tropospheric concentrations of trace species as the last scattering point for the photons received by the instrument is much lower in the atmosphere and is horizontally displaced from the instrument, giving a longer tropospheric absorption path (see for example Hönninger et al., 2004b).

Much work to date has concentrated on the measurement of background concentrations of NO_2 and halogen species in remote rural or polar regions (Frieß et al., 2001; Wittrock et al., 2004). For such measurements the temporal resolution of the instrument is not a primary concern as concentrations are expected to change over timescales of hours or days rather than minutes. As such, consecutive measurements from different viewing geometries are appropriate with a total scan of all viewing axes taking several minutes. However, for analysis of rapidly varying and spatially inhomo-

geneous concentrations of trace species in the boundary layer, simultaneous measurement of all viewing angles is highly desirable.

This paper describes the application of a concurrent multi-axis DOAS (CMAX-DOAS) system that measures five or more viewing geometries simultaneously and has been tested in urban conditions to measure the concentration and time evolution of boundary-layer nitrogen dioxide (NO_2).

2 Experimental

The CMAX-DOAS instrument was installed on the roof of the Space Research Centre at the University of Leicester (52.62° N, 1.12° W) at the end of 2003. The instrument is described in detail in Leigh et al. (2006). A clear view to the North was available, unobstructed by tall buildings and trees. The location of the installation in respect to the town centre and main traffic routes is shown in Fig. 1. Also shown in Fig. 1 are modeled mean annual NO_2 concentrations in the Leicester Area, and the location of 8 automated monitoring stations, operated by the local City Council. The northerly-pointing off-axis views sampled air masses over the main urban city centre in Leicester. The heterogeneity of the air-masses sampled by the different viewing directions limited the profiling capabilities of the CMAX-DOAS instrument using existing techniques. However, the concurrent nature of the multi-axis measurements can provide simultaneous analysis of different air-masses.

3 Results

The instrument was operated on 124 days during 2004 with a 2 min temporal resolution. An example set of daily data from 20 May 2004 is shown in Fig. 2. These data demonstrate the ability of the CMAX-DOAS system to concurrently measure NO_2, O_4, O_3 and H_2O. For analysis, the reference spectrum from the zenith view was used as reference for the off-axis views, providing maximum spatial information.

ACPD
6, 12671–12700, 2006

The stratospheric dominance of the ozone signal can be seen in the lack of dependence of measurement on viewing geometry, with a slant column purely dependent upon solar zenith angle. The NO_2 and O_4 slant columns demonstrate both tropospheric and stratospheric signals while the H_2O signal as expected is dominated by tropospheric signal. The constant and known profile of O_4 permits information to be obtained on the abundance of cloud or haze on a given day (Wagner et al., 2004). Clouds and haze influence photon path lengths by altering atmospheric scattering properties. While thick clouds can increase path lengths through increased scattering between and within clouds, thin cloud or haze will reduce path lengths in off-axis measurements, as scattering of photons is more likely to occur near the CMAX-DOAS instrument. Therefore, on this day, the O_4 slant columns indicate light non-uniform cloud as shown by the non-smooth curves, and the proximity of measurements from different axes. More cloud and haze effects are evident in the morning than the evening where dusk measurements almost resemble clear-sky conditions.

The NO_2 slant column contains information on stratospheric NO_2, contained in the solar zenith angle dependence of measurements at dawn and dusk, particularly in the zenith measurement which is least influenced by tropospheric concentrations. The diurnal increase in stratospheric NO_2 can be seen in the increased SZA dependence in the dusk measurements over dawn. In addition, tropospheric concentrations are clearly evident in the separation of the off-axis signals, and short temporal features. Path length changes indicated in O_4 measurements will also influence NO_2 measurements. For example, in Fig. 2 cloudy features appearing in the O_4 columns at 10:00 a.m. and 03:00 p.m. also appear as enhancements in the NO_2 slant columns.

Slant column data were produced for all 124 days on which measurements were taken. Short and long-term analysis was therefore possible to investigate individual features and establish diurnal, weekly, seasonal and annual concentrations. In order to build up a long time series of tropospheric NO_2 concentrations, a simple algorithm was developed to convert the CMAX-DOAS measurements into volume mixing ratios. This algorithm relies on the following assumptions:

ACPD
6, 12671–12700, 2006

EGU

1. The absorption by NO_2 outside of the polluted boundary layer is the same from both the zenith and off-axis viewing geometries.

2. Clouds when present are a uniform layer above the polluted boundary layer PBL, and scattering causing increased absorption is identical in both the zenith and off-axis views.

3. The 5° viewing angle samples a 2 km path of the polluted boundary layer, which is not sampled by the zenith view.

4. The concentration of NO_2 in the urban boundary layer is taken as the average concentration along this 2 km additional off-axis path photon path length.

The four assumptions made are summarised schematically in Fig. 3.

The validity of assumptions 1 and 2 are a function of the ratio of the concentrations of NO_2 within and beyond the urban boundary layer as well as the scattering properties of the atmosphere. With a cleaner background air mass, or higher concentrations of NO_2 in the urban boundary layer, the influence of differing absorption properties outside the area to be studied is reduced. The accuracy of assumptions 3 and 4 relates to the nature of the temporal and spatial variability in emissions, topography, and the dynamical progression of the air mass being measured. Both these assumptions have significant uncertainty and can be used as an adjustable parameter, however they provide a demonstration of technique, and in the future could be significantly improved through the incorporation of a second (orthogonal) instrument in the analysis.

From the application of the stated assumptions, the following algorithm can be derived for the average concentration of the polluted boundary layer along the line of sight of the instrument in $\mu g\,m^{-3}$:

$$\mathrm{Conc}_{\mathrm{PBL}} = \frac{SC^{OA}_{\mathrm{RTrop}}}{I_{ad} \bullet CF} \quad (1)$$

ACPD
6, 12671–12700, 2006

EGU

Where SC^{OA}_{RTrop} is calculated from the slant column derived from the off-axis measurements using a noon reference spectrum from the zenith. The slant column density measured by the zenith view at the same time is then removed to leave the residual off-axis column density, SC^{OA}_{RTrop},

l_{ad} = 2×10^5 and is the number of cm of additional path length and

CF = 1.29×10^{10} and is the conversion factor from mol cm^{-3} to μg m^{-3} for NO_2.

Derived concentrations using equation 1 from a period in May, and August 2004 are shown in Fig. 4. Although the absolute concentration derived using Eq. (1) is directly dependent upon the path length chosen, the diurnal and weekly variability are completely independent of the four stated assumptions, and therefore give a reliable indication of the sensitivity of the technique when compared with data from an in situ monitor. The in situ monitor selected for this exercise is located between two large buildings at the location marked "AUN" in Fig. 1. This location is selected to obtain an urban background without dominant influences from any single road, junction or industrial emission.

The data in Fig. 4 demonstrate the level of agreement between the CMAX-DOAS measurements and those from a chemiluminescence detector over a period of a few weeks. The weekly cycle is clearly evident, with the lowest concentrations from both instruments measured on the three Sundays. Given the difference in spatial sampling of the two measurements, the degree of agreement is significant. The absolute concentrations measured by the CMAX-DOAS instrument are directly dependent upon the path-length assumption used in Eq. (1). However, the trends are not dependent upon any assumptions made, and are directly derived from the DOAS fit. The reproduction of the weekly trend, and the identification of short-term features is therefore a significant piece of evidence that the CMAX-DOAS method is able to measure the NO_2 concentration in the polluted urban boundary layer, directly measuring the times and relative intensities of emission events. From Friday 7 May to Tuesday 11 May, morning and evening rush hours can be seen on week days, with lower concentrations and different

diurnal patterns evident during Saturday and Sunday.

From all the data collected it is possible to derive average concentrations for a given time on a given day of the week. Figure 5 shows 30 min binned average concentrations from all available CMAX-DOAS data in 2004. The normal diurnal and weekly anthropogenic cycles are evident in these data.

Wind data combined with the CMAX-DOAS dataset gives information on the influence of prevailing wind conditions on urban air quality, and the causes of differences between measurements by the in-situ chemiluminescence monitor and the CMAX-DOAS instrument. Figure 6 shows data from all periods in which CMAX-DOAS and chemiluminescence measurements were available concurrently (a total of 1412 hourly data points). The influence of wind direction on average NO_2 concentrations can be clearly seen with winds from the East of the city leading to the lowest measurements from both techniques. The influence of the CMAX-DOAS viewing geometry can be seen in data during southerly winds. A southerly wind will naturally disperse city centre emissions to the north of the city, away from the CMAX-DOAS instrument. As the CMAX-DOAS instrument's viewing geometry is inclined, polluted air masses are sampled later and at a higher altitude in southerly winds, or may possibly not be sampled at all. This is the reason for the distinct difference between CMAX-DOAS measurements and chemiluminescence data in southerly wind directions. However, the good agreement in all other wind conditions suggests that even with the use of only 2 viewing geometries from a single measurement location south of a city centre, the concentration of NO_2 in the air mass over the city can be reliably determined using the CMAX-DOAS system.

Analysis of a rare clear-sky morning period on 17 January 2004 is used to demonstrate the potential of the CMAX-DOAS instrument to gain information about the dynamical progression of individual air masses. For this analysis the DOAS retrieval was adapted, with the noon reference spectrum from each individual axis being used as the reference for the spectra from that axis, instead of using the zenith reference for all analysis. This method loses certain information on the vertical profile of the gases,

but also removes any influence of the changing instrument line shape over the surface of the CCD (Leigh et al., 2006). Therefore, residuals on all axes were reduced for the 1 min analysis to between 1.3‰ for the zenith view and 0.61‰ for the 15 degree elevation. Application of this analysis technique also permitted the use of a 2 degree viewing angle which was unreliable in the initial analysis owing to its low intensity and differences in instrument line shape compared to the zenith view.

Figure 7 shows the morning period between 09:20 and 09:50 a.m. with an expanded time axis. The data in Fig. 7 show distinct peaks indicative of the presence of discrete plumes of NO_2 in the viewing direction of the instrument.

The analysis of the finer structure of these peaks provides information on the transport of two plumes, their spatial extent, and their concentration of NO_2. The wind speed on the 17 January 2004 was approximately 1.6 m s^{-1} coming from a northerly direction. As the instrument is placed to the south of the city centre, plumes originating from the city centre are transported sequentially through each viewing direction of the CMAX-DOAS instrument. This progression through the viewing geometries can be clearly seen. Owing to the nature of the recording cycle in the CCD to PC interface, a measurement is missed every 6 to 10 min. In this time period, measurements are missing at 09:22, 09:29, 09:33 and 09:42. The missing measurements at 09:29 and 09:42 are particularly unfortunate in this particular case as they coincide with the two peaks, and cautious interpolations of the peak shapes around these missing points need to be made.

Information on these plumes can be gained from the amplitude of the peaks, their width, and the temporal shift between the appearance in each viewing direction. These parameters are listed in Table 1.

A relatively straightforward geometric analysis can be performed given four assumptions. The first assumption is that the wind speed is constant over the spatial and temporal domain. The wind speed is taken from the Leicester City Council meteorological station, which measures wind speed hourly. The 9 am reading was 1.8 m s^{-1}, the 10:00 a.m. reading was 1.4 m s^{-1}. Therefore the assumed wind speed for the pe-

riod around 09:30 a.m. is 1.6 m s^{-1}. The second assumption which is necessary is a vertical uplift rate for the plume. In the absence of information required for quantitative calculation of the plume rise rate using the Briggs equations (Briggs, 1975) such as emission speeds and temperatures, a rough estimation of 25 cm per second, or 10° in a 1.6 m s^{-1} wind was used. The third assumption is that the plume is spherical in such a slow wind. Such a simplistic assumption will introduce quantification errors, however future instrumental developments involving additional viewing geometries will allow the plume shape to be more accurately assessed. For this first demonstration the mathematical simplicity gained by such simple assumptions is paramount in the absence of significant additional plume shape information.

The final assumption required is that the plume is traveling directly towards the instrument and the centre of the plume is sampled by the off-axis and zenith geometries. Given the instrument position to the south of the city centre, and a measured Northerly wind, this assumption is acceptable within the parameters of this initial analysis.

These assumptions establish a relatively simple triangular geometry of the plume through the viewing angles of the CMAX-DOAS instrument, as illustrated in Fig. 8.

From this geometry several properties of the plume can be estimated. Firstly the dimension of the plume perpendicular to the line of sight from the instrument can be estimated from the time taken for it to be blown through that viewing direction at a given wind speed. This can be expressed as:

$$D(\theta) = U \bullet (T_f(\theta) - T_s(\theta)) \quad (2)$$

where

$$U = \sqrt{W^2 + R^2} \quad (3)$$

ACPD
6, 12671–12700, 2006

EGU

$D(\theta)$ = plume diameter when passing through a given viewing angle.
U = plume speed along its line of transport
$T_s(\theta)$ = start time of plume measurement from a given viewing angle
$T_f(\theta)$ = finish time of plume measurement from a given viewing angle
W = Wind speed as measured by in situ monitors
R = estimated plume rise rate.

The distance traveled between detection by subsequent viewing geometries can also be estimated through calculation of the distances CD, DE, EF, and FG.

For example

$$FE = \left(T_p(\theta_3) - T_p(\theta_2)\right) \bullet U \tag{4}$$

where:

FE is the distance between points F and E in Fig. 8.

$T_p(\theta_3)$ = is the time of peak plume intensity from viewing angle 3.

Once the distance FE has been calculated, the triangle AFE can be solved, calculating distances to the plume centres when the peak concentrations are being measured.

$$AF = \frac{\left(\sin\left(5^\circ\right) \bullet FE\right)}{\sin\left(155^\circ\right)} \tag{5}$$

Using the elevation angles of each viewing geometry and the calculated distance of the plume from the instrument, the horizontal (H^{AF}) and vertical (V^{AF}) displacement of the centre of the plume can be calculated at the time $T_p(\theta_3)$.

$$V^{AF} = \sin(15^\circ) \bullet AF \tag{6}$$

$$H^{AF} = \cos(15^\circ) \bullet AF \tag{7}$$

The maximum absorption of the plume can be measured from the amplitude of the plume peak above the background NO_2 concentration. Given the assumption that most

ACPD
6, 12671–12700, 2006

photons are scattered behind the plume, the absorption path length through the plume can be initially estimated using an assumed spherical plume shape where the absorption path is equal to the measured plume diameter $D(\theta)$. The average concentration in mol cm^{-3} within the plume can be calculated from:

$$N_\theta = \frac{A_\theta}{D(\theta)} \quad (8)$$

where A_θ is the amplitude of the peak as measured by a the view geometry with elevation angle θ (mol cm^{-2}).

The results of these calculations therefore provide estimations of the size of the plume, its position, and its concentration. Even with the assumption of spherical plumes, a first approximation of plume concentrations can be derived. However, the weakness of the assumption is evident as the plume concentration is calculated to decrease significantly as the plume is measured by the zenith view. This is chemically inconsistent with existing knowledge of urban NO_2 chemistry, and a much more likely scenario is a shallower, flatter plume which for a given concentration would cause a smaller amount of absorption in the vertical plane than the horizontal. The possibility that the zenith view is only measuring the edge of the plume must also be considered. The assumption that at each stage we are measuring the centre of the plume is a considerable one, especially as the calculated distance between the 15° measurement and the zenith measurement is 600 to 800 m. It is very likely that to some degree the zenith measurements for both plumes are lower due to the plume being blown through the off-axis viewing geometries and then to the side of the instrument rather than directly overhead. Without the use of additional azimuthal geometries it is difficult to quantify the extent of this effect.

Adjusting the assumption of spherical plumes to allow for a more elliptical geometry permits a more realistic modeling of likely plume dimensions. Using an assumed eccentricity, the path length through a plume with an elliptical cross section can be determined and used in concentration calculations. The path length through the plume from a given viewing geometry is dependent upon the elevation angle of that geometry

ACPD
6, 12671–12700, 2006

EGU

and the eccentricity of the ellipse. The eccentricity of the ellipse is defined as:

$$\varepsilon = \sqrt{1 - \left(\frac{Y}{X}\right)^2} \quad (9)$$

With wind fields of 1.6 m s^{-1} horizontally, and 0.25 m s^{-1} vertically, an Y/X value of 0.2 was used as an initial estimation of plume shape. An intermediate step using Y/X of 0.4 was also calculated to provide a measure of the sensitivity of calculated concentrations to this Y/X factor. Results from these calculations, including estimated plume positions, dimensions and concentrations at each of the 5 points at which the plume is sampled, are shown in Fig. 9.

3.1 Source location and strength estimation

The total mass of NO_2 in the plumes can be roughly estimated through calculation of the volume of the elliptical plumes. If the assumption is made that the concentration is constant throughout the plume, and that the elliptical plume has the same dimensions in the vertical and East-West dimension, then the total mass of NO_2 within the plume can be calculated for any of the ellipses drawn in Fig. 9.

For example, for plume 1 (see Table 1) measured by the 15° elevation angle, using an assumed Y/X factor of 0.2, the measured diameter is 877 m, and the concentration is 26 ppbV. Therefore the total mass of NO_2 in that plume, given the above assumptions can be calculated as follows:

Total Volume = $\frac{4}{3}\pi \times (877 \times 0.5) \times (877 \times 0.4 \times 0.5) \times (877 \times 0.4 \times 0.5) = 1.46 \times 10^7$ m^3

1 ppbV = 1.913 μg m^{-3}

26 ppbV = 49.738 μg m^{-3} = 4.974×10^{-8} kg m^{-3}.

Therefore the total mass of NO_2 in the plume = $4.974 \times 10^{-8} \times 1.46 \times 10^7 = 0.73$ kg. This is a significant mass of NO_2, which would require a repeated and distinct emission source. The estimated source position can be estimated by extrapolating back from the

measured plume positions from the different axes and calculating the distance AB in Fig. 8. For both plumes the source location is calculated to be between 1.2 and 1.4 km to the north of the CMAX-DOAS instrument.

The main train station in Leicester is located approximately 1.3 km to the north of the site of the CMAX-DOAS instrument. The acceleration of diesel trains out of the station is therefore a possible source of such significant plumes.

As a further demonstration of capability, two additional viewing geometries were temporarily added to the CMAX DOAS instrument on 11 November 2004. These geometries were at 15° elevation angle, with one telescope pointing at 20° and the other at 340° 2° azimuthal angles (i.e. One telescope 20° east of the permanent view geometries, and one 20° west). These additional viewing geometries permitted the tracking of individual plumes as they were blown by a westerly wind through the different viewing geometries.

The use of 7 concurrent fibres necessitated the concentration of the images on the CCD chip. Normal operation with 5 fibres used alternate inputs into the 9-way mutli-track fibre giving a spacing between images of approximately 100 rows, and negligible stray-light concerns. This configuration therefore not only tested the utility of the additional viewing geometries, but also the capability of the CCD and spectrometer system to accommodate additional viewing geometries.

Clear sky conditions were available during the morning period around 08:00 a.m., when the wind direction was approximately 210° with an average wind speed of $1.5\,m\,s^{-1}$. Therefore, plumes detected around this time would be traveling from the South West to the North East at approximately $1.5\,m\,s^{-1}$. Slant columns of NO_2 from the available azimuthal angles are shown in Fig. 10. Reference spectra from each viewing angle were used, rather than using a single zenith reference spectrum. Three pollution peaks were observed between 07:00 and 09:00 a.m. Three plumes can be seen to progress through the Westerly view, the northerly-viewing geometries, and finally the most Easterly telescope. O_4 slant columns for the same period are shown in Fig. 11 demonstrating that although there is some structure, suggesting a little cloud

ACPD
6, 12671–12700, 2006

EGU

cover on this particular morning, there are not the three distinct structures observed in the NO_2 data.

The irregular shapes of these three plumes render the analysis problematic given such minimal constraining data points. Initial information is available from the plume amplitudes, which are approximately 2×10^{16} mol cm^{-2}, therefore these plumes are less concentrated than plume 1 in Fig. 7 from 17 January 2004. With a wind speed of 1.5 m s^{-1} at 210° the components of the wind speed in the South-North, and West-East directions are 1.3 and 0.75 m s^{-1} respectively. Transit times of 4–6 min through the viewing geometries give an initial estimation of diameter of 720 m. Gaps of approximately 1 min between peak detection in the azimuthal directions for all 3 peaks gives an estimated distance from the instrument of approximately (60×0.75)/tan 20=125 m. With the incorporation of additional viewing geometries or an increase in temporal resolution, more information on plume dimensions and concentrations could be gained.

4 Conclusions

Sensitivity tests have demonstrated the reliability of fine structure visible in slant columns measured in urban environments with the CMAX-DOAS instrument. (Leigh et al., 2006) Through the use of a simple geometric, information on trace gas concentrations in an urban atmosphere can be derived from concurrent measurements. Such tropospheric measurements provide a measure of the integrated concentration of the trace species along a path above the city centre. These measurements therefore provide a useful measure of overall trace gas concentrations on a city-wide scale. In northerly wind conditions these measurements compare well with a chemiluminescence monitor placed in a sheltered location in the city centre. Such agreement confirms the ability of both instruments to retrieve reliable measurements of NO_2 concentrations over a moderately-sized urban area with a multitude of individual sources.

By analysing this fine structure, individual plumes of NO_2 can be identified as they are blown through the instrument viewing geometries. The concurrent nature of the

measurements from the CMAX-DOAS instrument enables limited spatial information to be derived from peaks which are visible in multiple axes.

In favourable wind conditions, in which the original source of the plume is directly downwind of the instrument, a simplified geometry can be used to reconstruct plume dimensions, concentrations and source location. This simplified geometry makes numerous assumptions owing to the very limited spatial information available. However, despite the significant assumption uncertainties, derived plume dimensions and concentrations are within expected parameters and likely source locations can be identified.

The CCD and imaging spectrometer system demonstrated in this work is capable of accommodating up to a total of 20 viewing geometries, with minimal stray light problems caused by a 50-row separation between imaged spectra. Additional azimuthal telescopes could be used to track the spatial extent and transit of plumes in all wind conditions. With only 2 additional azimuthal telescopes, the amount of spatial information is very limited. However, the irregular plume shapes expected, and suggested by initial investigations demonstrate the utility of each additional view. With the development of the next generation of instrument incorporating 20 fixed telescopes the amount of spatial and temporal information available increases significantly. Using two or more instruments with intersecting viewing geometries would constrain the depth dimension of analysed plumes. The extension of techniques demonstrated in this work into multiple instruments with intersecting viewing geometries can be seen as a way of imaging city-scale import, emission and export.

Acknowledgements. The authors would like to thank Leicester City Council for provision of wind field and chemiluminescence data. We are also grateful to NERC for funding this project under contract NER/S/A/06294.

References

Aliwell, S. R., Van Roozendael, M., Johnston, P. V., Richter, A., Wagner, T., Arlander, D. W., Burrows, J. P., Fish, D. J., Jones, R. L., Tornkvist, K. K., Lambert, J. C., Pfeilsticker, K.,

and Pundt, I.: Analysis for BrO in zenith-sky spectra: An intercomparison exercise for analysis improvement, J. Geophys. Res.-Atmos., 107, 4199, doi:10.1029/2001JD000329, 2002. 12673

Bobrowski, N., Hönninger, G., Galle, B., and Platt, U.: Detection of bromine monoxide in a volcanic plume, Nature, 423, 273–276, 2003. 12673

Briggs, G.: Plume rise predictions, lectures on Air Pollution and Environmental Impact Analysis, Tech. rep., U.S. Dept of Energy, 1975. 12680

Frieß, U., Wagner, T., Pundt, I., Pfeilsticker, K., and Platt, U.: Spectroscopic measurements of tropospheric iodine oxide at Neumayer Station, Antarctica, Geophys. Res. Lett., 28, 1941–1944, 2001. 12673

Heckel, A., Richter, A., Tarsu, T., Wittrock, F., Hak, C., Pundt, I., Junkermann, W., and Burrows, J. P.: MAX-DOAS measurements of formaldehyde in the Po-Valley, Atmos. Chem. Phys., 5, 909–918, 2005, http://www.atmos-chem-phys.net/5/909/2005/. 12673

Hönninger, G., Bobrowski, N., Palenque, E. R., Torrez, R., and Platt, U.: Reactive bromine and sulfur emissions at Salar de Uyuni, Bolivia, Geophysical Research Letters, 31, L04101, doi:10.1029/2003GL018818, 2004a. 12673

Hönninger, G., Leser, H., Sebastian, O., and Platt, U.: Ground-based measurements of halogen oxides at the Hudson Bay by active longpath DOAS and passive MAX-DOAS, Geophys. Res. Lett., 31, L04111, doi:10.1029/2003GL018982, 2004b. 12673

Hönninger, G., von Friedeburg, C., and Platt, U.: Multi axis differential optical absorption spectroscopy (MAX- DOAS), Atmos. Chem. Phys., 4, 231–254, 2004c. 12673

Johnston, P. V. and McKenzie, R. L.: NO_2 Observations at 45-Degrees-S During the Decreasing Phase of Solar-Cycle 21, from 1980 to 1987, J. Geophys. Res.-Atmos., 94, 3473–3486, 1989. 12673

Leigh, R. J., Corlett, G. K., Frieß, U., and Monks, P. S.: A Concurrent Multi-Axis Differential Optical Absorption Spectroscopy system for the Measurement of Tropospheric Nitrogen Dioxide, Appl. Opt., 45, 7504–7518, 2006. 12674, 12679, 12685

Leser, H., Hönninger, G., and Platt, U.: MAX-DOAS measurements of BrO and NO_2 in the marine boundary layer, Geophys. Res. Lett., 30, 1537, doi:10.1029/2002GL015811, 2003. 12673

Miller, H. L., Weaver, A., Sanders, R. W., Arpag, K., and Solomon, S.: Measurements of arctic sunrise surface ozone depletion events at Kangerlussuaq, Greenland (67 degrees N, to 51 degrees W), Tellus Ser. B-Chem. Phys. Meteorol., 49, 496–509, 1997. 12673

Noxon, J. F.: Nitrogen Dioxide in the Stratosphere and Troposphere measured by Ground-based absorption spectroscopy, Science, 189, 547–549, 1975. 12673

Noxon, J. F., Whipple, E. C., and Hyde, R. S.: Stratospheric NO2, 1. Observational method and behaviou at Midlatitudes, J. Geophys. Res.-Atmos., 84, 5047–5076, 1979. 12673

Platt, U.: Differential optical absorption spectroscopy, (DOAS), in air monitoring by spectroscopic techniques, in: Chemical Analysis, edited by: Sigrist, M. W., vol. 127, Wiley, New York, 1994. 12673

Sanders, R. W.: Improved analysis of atmospheric absorption spectra by including the temperature dependence of NO_2, J. Geophys. Res.-Atmos., 101, 20 945–20 952, 1996. 12673

Sinreich, R., Volkamer, R., Filsinger, F., Frieß, U., Kern, C., Platt, U., Sebastián, O., and Wagner, T.: MAX-DOAS detection of glyoxal during ICARTT 2004, Atmos. Chem. Phys, 6, 9459–9481, 2006. 12673

Solomon, S., Schmeltekopf, A. L., and Sanders, R. W.: On the Interpretation of Zenith Sky Absorption-Measurements, J. Geophys. Res.-Atmos., 92, 8311–8319, 1987. 12673

Tornkvist, K. K., Arlander, D. W., and Sinnhuber, B. M.: Ground-based UV measurements of BrO and OClO over Ny-Alesund during winter 1996 and 1997 and Andoya during winter 1998/99, J. Atmos. Chem., 43, 75–106, 2002. 12673

Van Roozendael, M., Hermans, C., Demaziere, M., and Simon, P. C.: Stratospheric NO2 observations at the Jungfraujoch Station between June 1990 and May 1992, Geophys. Res. Lett., 21, 1383–1386, 1994. 12673

Wagner, T., Dix, B., von Friedeburg, C., Friess, U., Sanghavi, S., Sinreich, R., and Platt, U.: MAX-DOAS O-4 measurements: A new technique to derive information on atmospheric aerosols - Principles and information content, J. Geophys. Res.-Atmos., 109, D22205, doi:10.1029/2004JD004904, 2004. 12675

Wittrock, F., Muller, R., Richter, A., Bovensmann, H., and Burrows, J. P.: Measurements of iodine monoxide (IO) above Spitsbergen, Geophys. Res. Lett., 27, 1471–1474, 2000. 12673

Wittrock, F., Oetjen, H., Richter, A., Fietkau, S., Medeke, T., Rozanov, A., and Burrows, J. P.: MAX-DOAS measurements of atmospheric trace gases in Ny-Alesund - Radiative transfer studies and their application, Atmos. Chem. Phys., 4, 955–966, 2004, http://www.atmos-chem-phys.net/4/955/2004/. 12673

Table 1. Details of the two pollution peaks shown in Fig. 7.

	Peak1			Peak2		
Viewing Direction	Amp	Width	Time	Amp	Width	Time
2°	2.2	6.5	09:29:00	1.0	4.0	09:38:30
5°	6.5	9.5	09:31:00	3.0	6.6	09:40:30
10°	7.0	8.5	09:32:00	3.0	5.5	09:42:30
15°	5.5	9.0	09:34:00	2.5	5.5	09:44:00
Zenith	1.0	4.0	09:37:00	0.5	3.5	09:45:30

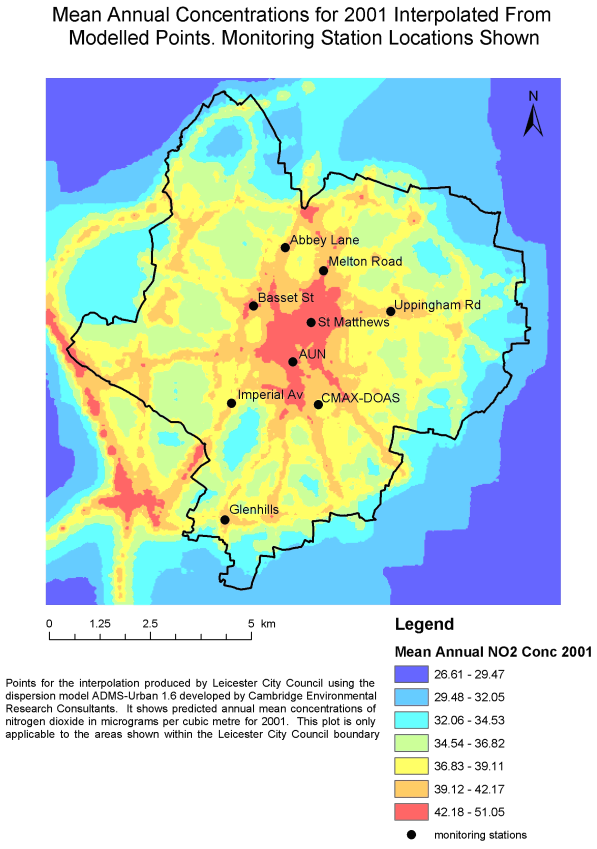

Fig. 1. Modeled NO_2 concentrations in the Leicester Area, produced by the ADMS model, using assimilated data from the automated monitoring stations marked on the map. The location of the CMAX-DOAS instrument is shown.

ACPD
6, 12671–12700, 2006

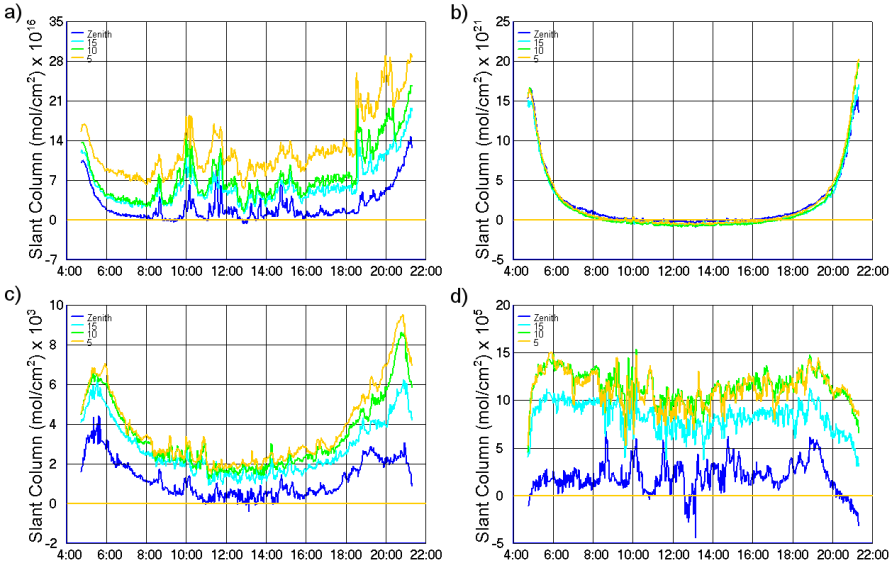

Fig. 2. Slant columns for all retrieved absorbers from Thursday 20th May 2004 for all viewing axes. Panels are: **(a)** NO_2, **(b)** O_3, **(c)** O_4, **(d)** H_2O.

ACPD
6, 12671–12700, 2006

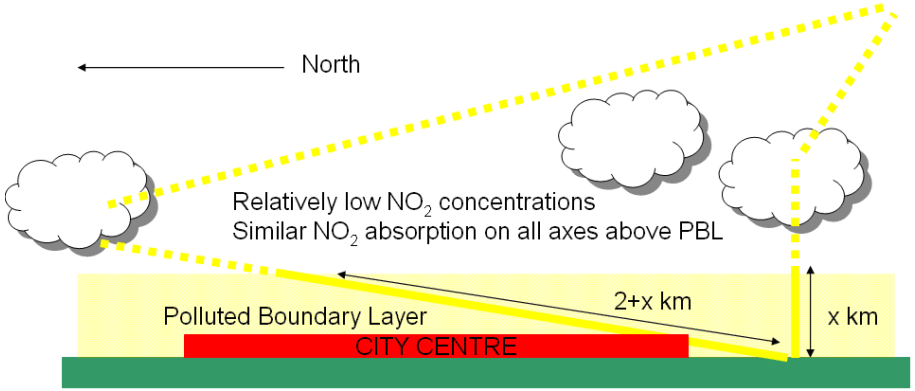

Fig. 3. Schematic representation of the assumptions made in troposperhic column calculations. Absorption on all axes is assumed to be similar above the PBL, while within the PBL the off-axis view has an additional 2 km path length through the PBL.

ACPD
6, 12671–12700, 2006

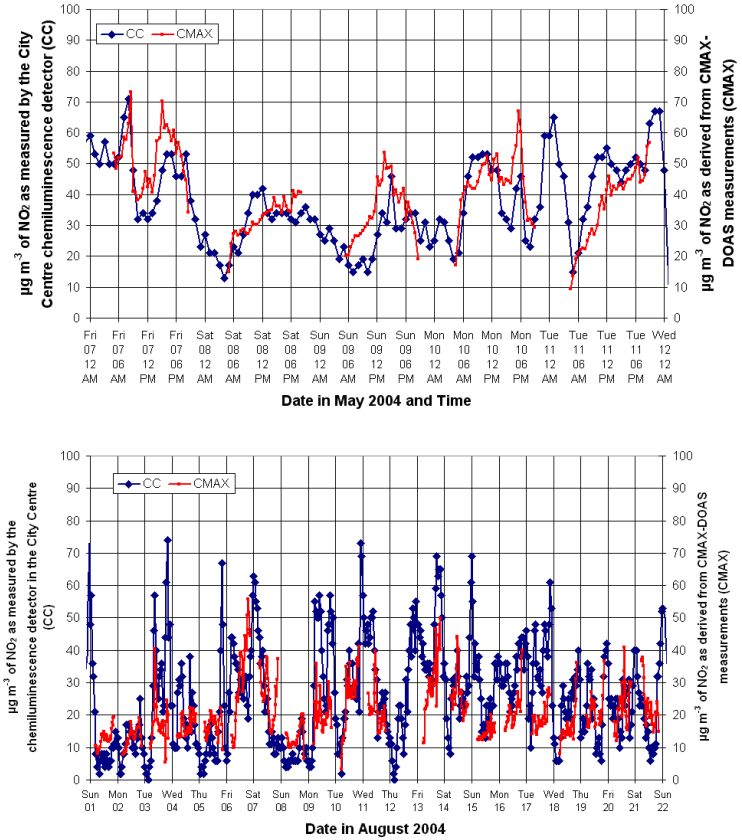

Fig. 4. Derived tropospheric concentrations from the CMAX-DOAS instrument, and data from the in-situ chemiluminesence monitor for two periods in May and August 2004.

ACPD
6, 12671–12700, 2006

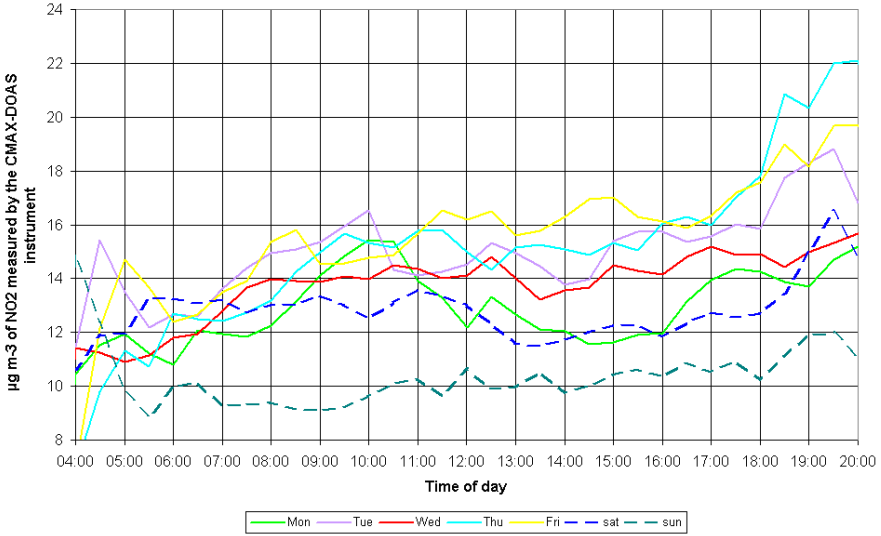

Fig. 5. Average concentrations of NO_2 for each day of the week as measured by the CMAX-DOAS instrument over Leicester during 2004.

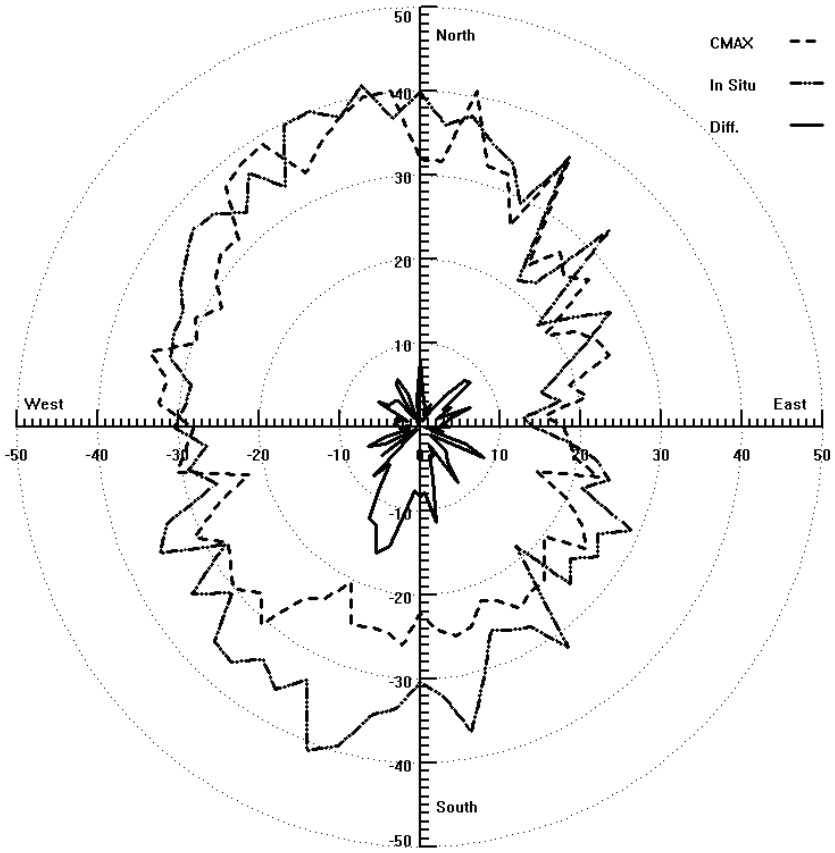

Fig. 6. Annual average NO_2 concentrations for a given wind direction from CMAX-DOAS measurements, and the in-situ chemiluminesence monitor.

ACPD
6, 12671–12700, 2006

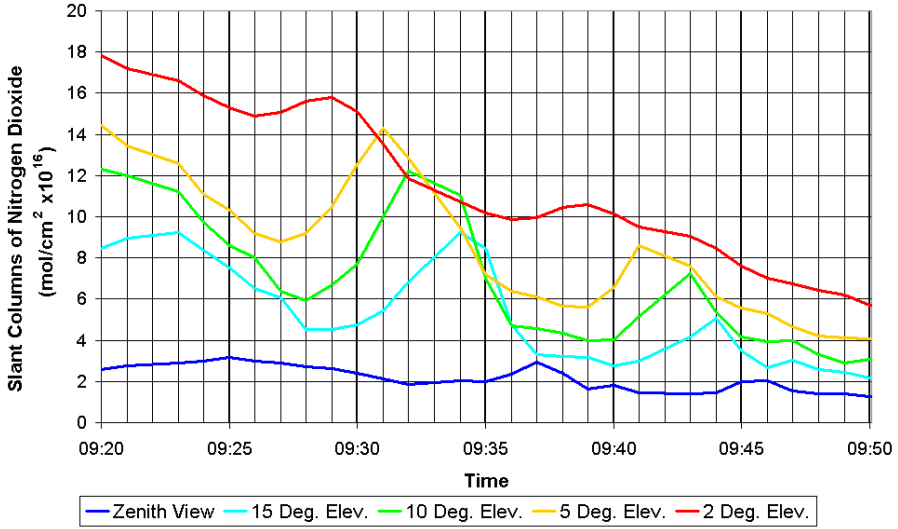

Fig. 7. Passing of two NO_2 pollution plumes on the morning of the 17 January 2004.

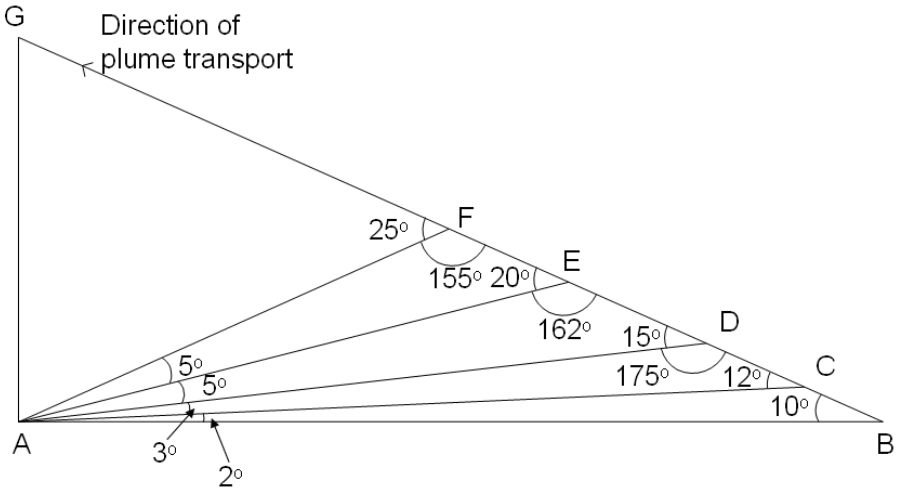

Fig. 8. Simplified geometry for plume analysis (see text).

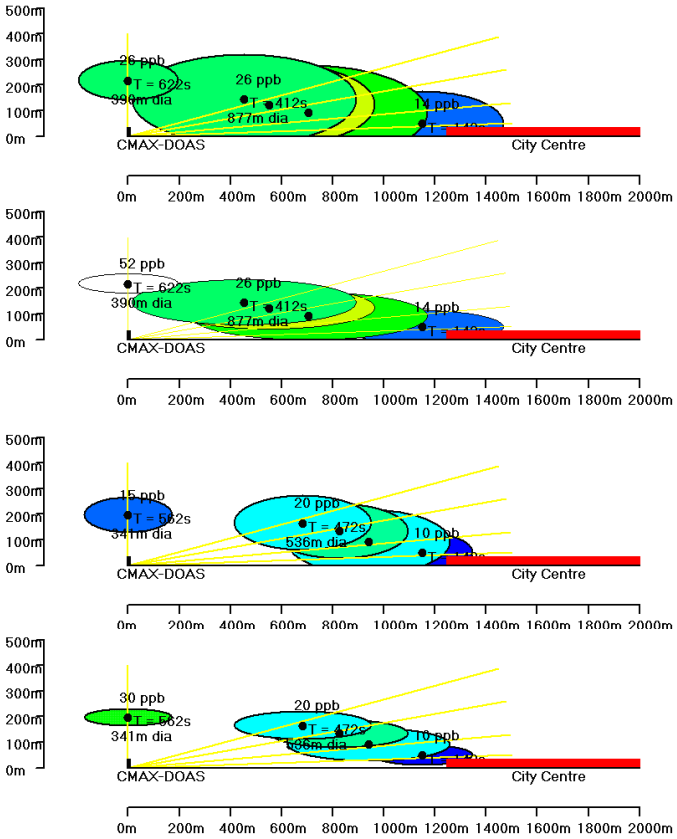

Fig. 9. Calculation of the positions and concentrations for plumes on 17 January 2004 (see Fig. 7) (plume 1 upper 2 panels, plume 2 lower two panels) using a Y/X ratio of 0.4 (top) and 0.2 (bottom).

ACPD
6, 12671–12700, 2006

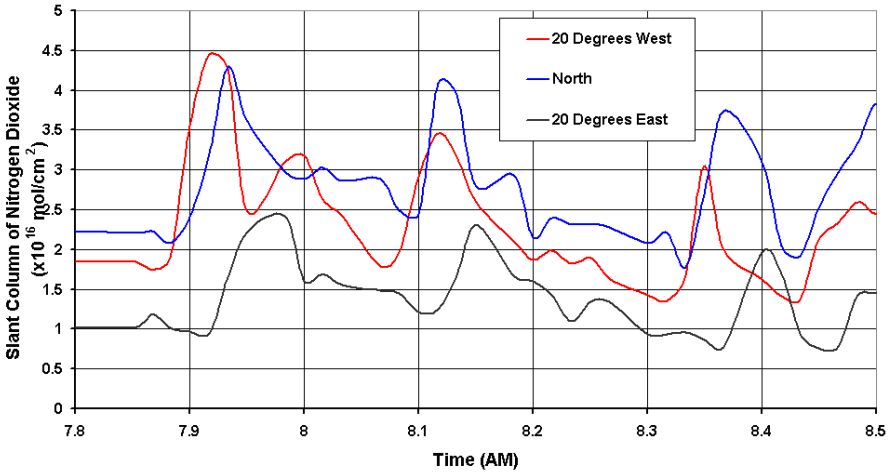

Fig. 10. Slant columns of NO_2 from the three telescopes at 15° elevation, showing the progression of three individual plumes as they progress from West to East.

ACPD
6, 12671–12700, 2006

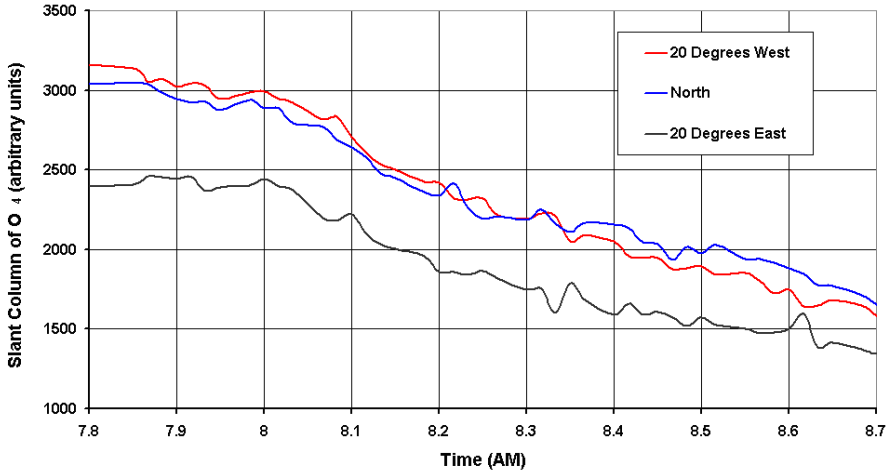

Fig. 11. Slant columns of O_4 for the morning of 11 November 2004, showing predominantly clear sky conditions.